Heliyon 10 (2024) e39133

Contents lists available at ScienceDirect

Heliyon

journal homepage: www.cell.com/heliyon

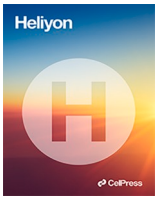

Research article

Cancer-associated fibroblasts-derived CXCL1 activates DEC2-mediated dormancy in oral squamous cell carcinoma

Wei-long Zhang [a,1], Hua-yang Fan [b,1], Bin-jun Chen [b], Hao-fan Wang [b], Xin Pang [b], Mao Li [a], Xin-hua Liang [b], Ya-ling Tang [a,*]

[a] State Key Laboratory of Oral Diseases & National Center for Stomatology & National Clinical Research Center for Oral Diseases & Dept. of Oral Pathology, West China Hospital of Stomatology, Sichuan University, Chengdu, 610041, Sichuan, China
[b] State Key Laboratory of Oral Diseases & National Center for Stomatology & National Clinical Research Center for Oral Diseases & Dept. of Oral and Maxillofacial Surgery, West China Hospital of Stomatology, Sichuan University, Chengdu, 610041, Sichuan, China

ARTICLE INFO

Keywords:
Oral squamous cell carcinoma
DEC2
Cancer-associated fibroblasts
Tumor dormancy

ABSTRACT

Cancer-associated fibroblasts (CAFs) are known to play an important role in cancer progression, but their effects on tumor cell dormancy and the underlying mechanisms remain to be explored. Here, we aimed to dissect the intercellular communication between CAFs and oral squamous cell carcinoma (OSCC) cells under cellular dormancy. In this study, we investigated 61 OSCC patients and found that low expression of Differentiated Embryonic Chondrocyte gene 2 (DEC2) was closely associated with tumor recurrence, cisplatin chemotherapy administration, and infiltration of CAFs. Overexpression of DEC2 promoted the invasion and migration ability of OSCC cells but inhibited their proliferation and glucose metabolism, and characterized them as dormant and cisplatin-resistant cells. C-X-C motif ligand 1 (CXCL1) from CAFs was found to down-regulate DEC2 expression in OSCC cells, ultimately awakening dormant cells and leading to tumor recurrence, which was validated *in vitro* and *in vivo*. In conclusion, CAFs-derived CXCL1 down-regulated DEC2 and "interrupted" DEC2-mediated OSCC cell dormancy, which may be a mechanism by which CAFs modulate OSCC cell dormancy and contribute to the development of new therapies for OSCC.

1. Introduction

Oral squamous cell carcinoma (OSCC) accounts for approximately 90 % of oral and maxillofacial malignancies [1]. Despite the significant advances in multiple treatments for OSCC, such as surgery, chemotherapy, radiotherapy, and immunotherapy, its five-year survival rate has been stagnant at approximately 50 % over the past decades [2], primarily attributed to late diagnosis, local recurrence, and distant metastasis [3,4].

Cancer dormancy has been reported to be the origin of cancer recurrence and metastasis, which refers to a protracted stage in cancer progression in which the disease remains undetected before bursting into a proliferative state [5]. Based on its molecular mechanisms, cancer dormancy is categorized into angiogenic dormancy, immune-mediated dormancy, and cellular dormancy [5]. Cellular dormancy is characterized by reduced metabolism and G0-G1 cell cycle arrest, rendering them resistant to chemotherapy and

* Corresponding author.
E-mail address: tangyaling@scu.edu.cn (Y.-l. Tang).
[1] These authors contributed equally to this work.

https://doi.org/10.1016/j.heliyon.2024.e39133
Received 27 January 2024; Received in revised form 3 September 2024; Accepted 8 October 2024
Available online 10 October 2024

determining chemotherapeutic efficacy [6]. However, under the influence of exogenous factors, dormant tumor cells can be reactivated and enter a state of rapid proliferation, which has been assumed as the source of tumor recurrence and metastasis [7].

Interactions between cancer cells and their tumor microenvironment (TME) are considered to regulate many aspects of tumor biology, including cell dormancy [8]. As one of the most abundant stromal cells within the TME, cancer-associated fibroblasts (CAFs) are critically involved in tumorigenesis, angiogenesis, metastasis, and drug resistance [9]. In addition, CAFs are found to be associated with tumor cell dormancy, for instance, they can affect cell dormancy by regulating autophagy in ovarian cancer [10]. However, direct evidence is urgently needed to determine the functional roles of CAFs in regulating OSCC cell dormancy and its underlying mechanisms.

Differentiated embryonic chondrocyte expressed gene 2 (DEC2) is an important member of the basic helix-loop-helix (bHLH) transcription factors family [11]. It regulates circadian rhythms and hypoxic stress, and is strongly associated with tumor proliferation, invasion, and chemotherapy resistance [12–14]. In addition, it was found that DEC2 was involved in the regulation of cell dormancy in head and neck squamous cell carcinoma (HNSCC), in which TGFβ2 induced tumor cell dormancy by activating the TGFβ/p38 axis and up-regulating the expression levels of DEC2 and p27 [15]. Furthermore, cytokines and chemokines produced by tumor cells or neighboring cells in the TME may be involved in the regulation of DEC2 expression [16]. Supernatants of CAFs have been found to up-regulate the expression of DEC1, a DEC2 homologous member, and to promote epithelial mesenchymal transition (EMT) and invasive ability of prostate cancer cells [17]. However, whether CAFs in the OSCC TME can regulate DEC2-mediated tumor dormancy or tumor reactivation and their intrinsic mechanisms remain unclear.

In the previous study, two different cell dormancy fates of salivary adenoid cystic carcinoma (SACC) were found based on the different expression of DEC2 in the primary and metastatic SACC. Different hypoxia states in primary and metastasis lesions may regulate DEC2-induced dormancy to keep or awaken the cell dormancy state [18]. In this study, we combined clinical specimens with *in vitro* and *in vivo* experiments to investigate the effects of DEC2 on cell dormancy and chemoresistance of OSCC cells, as well as the roles of CAFs in DEC2-mediated cell dormancy of OSCC cells and the potential mechanisms.

2. Materials and methods

2.1. Clinical samples collection

This study was approved by the Institutional Ethics Committee of West China Hospital of Stomatology of Sichuan University (approval no. WCHSIRB-D-2021-038). Informed consent was obtained from all enrolled patients. Formalin-fixed, paraffin-embedded tissue samples of 61 OSCC patients were collected from the Department of Oral Pathology, West China Hospital of Stomatology, Sichuan University, between 2010 and 2013. OSCC patients who received preoperative radiotherapy, hormone therapy, or non-cisplatin chemotherapy were excluded from this study. Of these 61 OSCC patients, 30 relapsed, 12 relapsed within 3 years, 8 relapsed between 3 and 5 years, and 10 relapsed after 5 years. The primary specimens from these patients constituted the OSCC tissue microarrays utilized in this study, and their recurrent specimens (not collected in the OSCC tissue microarrays) were obtained at their follow-up visits. Fresh human OSCC tissues and their corresponding normal tissues (at least 5 cm away from a tumor) were collected from OSCC patients without any radiotherapy or chemotherapy previously at the West China Hospital of Stomatology. Resected fresh OSCC and normal tissues were minced, digested in type I collagenase (Sigma, USA), and cultured in DMEM medium with 10 % fetal bovine serum (FBS; GIBCO, USA). The primary fibroblasts were purified, verified by immunofluorescence, and used before passage 6.

2.2. Immunohistochemistry (IHC), cell senescence detection, and terminal deoxynucleotidyl transferase-mediated dUTP-biotin nick end labeling (TUNEL) assay

Paraffin-embedded sections (4 μm) were deparaffinized in xylene and rehydrated, after which endogenous peroxidase was blocked using 3 % hydrogen peroxide. Paraffin-embedded sections were subjected to antigen retrieval by citric acid buffer (Agilent, USA). Next, these sections were incubated with primary antibodies (anti-DEC2, 1:100, Proteintech, USA; anti-Ki-67, 1:100, Servicebio, CN; anti-α-SMA, 1:100, Bimake, USA) and labeled with biotinylated goat anti-rabbit IgG (Zhongshan Goldenbridge Biotechnology, China). Finally, 3,3′-diaminobenzidine (DAB) was used to visualize proteins. The staining area was semi-quantified by software Image J 1.8.0. Senescent cells were detected by a senescence β-galactosidase staining kit according to the manufacturer's protocol in triplicate (Beyotime, China). Terminal deoxynucleotidyl transferase-mediated dUTP nick and labeling (TUNEL) Kit (KeyGEN, CN) was used to detect apoptotic cells of the OSCC tissues. Negative was graded as 0–10 % within 4–6 microscopic fields at × 400 magnification, and the positive was graded as more than 10 % as well.

2.3. Cloning, lentivirus preparation, and plasmids

For the constitutive over-expression of DEC2, the targeted sequence of DEC2 was cloned into the pEZ-Lv201/Puro vector, transfected into cells by polybrene (GeneCopoeia, USA) and selected with puromycin for 2 weeks according to the manufacturer's instructions.

2.4. Quantitative real-time (qRT)-PCR and western blot

Total RNA was extracted from cells using the RNAiso Plus (Takara, Japan), after which was examined by NanoDrop ND-1000

Spectrophotometer (ThermoFisher, USA). RNA was reverse transcribed to cDNA using the First-Strand Synthesis Kit (GeneCopoeia, USA) according to the manufacturer's user manual. BlazeTaq SYBR Green qPCR mix was used for qRT-PCR, and results were analyzed by Applied Biosystems ABI PRISM 7300. The primer sequences are listed in Table S1. Total proteins were extracted using a total protein extraction kit (KeyGEN, CN), and relative concentrations were quantified by a BCA Protein Assay Kit (Beyotime, CN). Protein samples were then separated by 8 % and 10 % sodium dodecyl sulfate-polyacrylamide gel electrophoresis (SDS-PAGE) at 80–120 V, transferred by wet electrophoresis (Bio-Rad, USA) onto polyvinylidene fluoride (PVDF) membranes and blocked by 5 % non-fat milk for 1 h at room temperature. Primary antibodies: DEC2 (Proteintech, USA), α-SMA (Bimake, USA), Vimentin (Bimake, USA), Ki-67 (Servicebio, CN), GAPDH (Signalway, USA), p21 (Cloud-Clone, CN), p27 (Bimake, USA), NR2F1 (Bimake, USA), MRP1 (Wanlei, CN), BCRP (Wanlei, CN), LRP (Wanlei, CN). Horse radish peroxidase-conjugated anti-rabbit or anti-mouse secondary antibody was used for subsequent visualization. The blots were visualized using the ChemiDoc^{TM} XRS + System (Bio-Rad, USA). Quantification of Western blot bands was calculated by ImageJ, and the expression level quantitation value is the ratio of the gray value of the target band to the corresponding GAPDH gray value.

2.5. Cell lines and cell culture

Human OSCC cell lines (CAL27 and SCC47) and Normal oral keratinocyte (NOK) cells were obtained from the State Key Laboratory of Oral Diseases of Sichuan University. CAL27 and SCC47 cells were cultured in Dulbecco's modified Eagle's medium (DMEM; Gibco, USA) with 10 % fetal bovine serum (FBS; Gibco, USA). NOK cells were cultured in Keratinocyte serum-free medium (K-SFM; Gibco, USA) with 10 % FBS. The cells were maintained at 37 °C with 5 % CO_2 atmosphere.

2.6. Wound Healing, Transwell Invasion, proliferation, cell cycle, apoptosis, and glucose consumption assay

For the Wound Healing assay, 6×10^5 CAL27 and SCC47 cells were counted and cultured in a 6-well plate. Upon reaching 90 % confluence, the wound was scratched by a pipette tip, and cultured in serum-free DMEM medium for 48 h. Phase-contrast microscopy ($\times$ 40) was used to take photographs at 0 and 48 h. The area of closed scratches was calculated using ImageJ software. Percent wound closure = (Initial Scratch Area - Scratch Area after 48 h)/Initial Scratch Area $\times$ 100 %.

For the Transwell Invasion assay, 1×10^5 CAL27 and SCC47 cells were resuspended in 200 μL serum-free DMEM medium and seeded into the upper chamber of an 8-μm-pore Transwell system coated with Matrigel (Corning, USA, 1:7.5). 500 μL DMEM medium with 10 % FBS was added into the lower chamber. After incubation for 24 h, OSCC cells that adhered to the upper surface of the filter were removed with a cotton swab. Then the cancer cells that invaded the Matrigel were stained with 0.5 % crystal violet and photographed under microscopy ($\times$ 200). The number of stained cells in five randomly selected areas was counted under a phase-contrast microscope to determine the average number of invading cells in a single experiment.

Cell proliferation was evaluated by CCK-8 assay. 3×10^3 CAL27 or SCC47 cells were seeded into 96-well plates in triplicate. After incubation for 24 h, 10ul CCK-8 solution (Apexbio, USA) was added to each well and incubated for 1.5 h at 37 °C. Cell viability was measured at 450 nm.

1×10^6 OSCC cells were collected, fixed with 70 % ethanol, and stained with propidium iodide (PI) using a Cell Cycle Detection Kit (KeyGEN, CN). Data was acquired with a Beckman Coulter flow cytometer. Annexin V-PE/7-AAD Apoptosis Detection Kit was used to differentiate apoptotic cells from viable or necrotic ones (SinoBiological, CN).

1×10^6 OSCC cells were collected and resuspended with 4 °C PBS. 100 μL suspensions were added to each labeled tube, followed by 10 μL Annexin V–PE and 10 μL 7-AAD, which was incubated in the dark for 20 min at room temperature. Finally, 400 μL PBS binding buffer was added to each tube and analyzed using FCM analysis (Biosciences Clontech, USA) for an hour.

The glucose consumption test was performed by a glucose assay kit according to the manufacturer's protocol in triplicate (Rsbio, CN).

2.7. Isolation and culture of CAFs and normal fibroblasts (NFs), immunofluorescence (IF)

Fresh OSCC tissues and para-cancerous tissues beyond 2 cm were placed in PBS solution containing 1 % penicillin-streptomycin solution (Hyclone, USA) and immersed for 5 min, which was repeated 3 times to remove residual blood and debris from the surface of the specimens. The washed specimens were cut into 1 mm^3 size and then digested with DMEM medium containing 0.5 % Collagenase IV (Sigma, USA) and 1 % penicillin-streptomycin solution and incubated for 4 h at 37 °C. Cell precipitates were collected and then resuspended in complete medium for cell culture. Spindle-shaped cells were observed crawling out under the microscope, which were CAFs and could be identified by IF. The isolation and culture process of NFs is similar to that of CAFs.

For IF staining, 5×10^4 NFs or CAFs were cultured in a 24-well plate for 24 h and then fixed with 4 % paraformaldehyde. After permeabilization with 0.25 % Triton X-100 for 15 min, cells were blocked with 1 % bovine serum albumin for 30 min. At last, cells were incubated with α-SMA antibody (1:50 dilution), vimentin (1:50 dilution), and TRITC-conjugated goat anti-rabbit IgG (1:500; Zhongshan Goldenbridge Biotechnology, CN). Olympus microscope (Tokyo, Japan) was used to visualize cells and take images.

2.8. Collection of conditioned medium (CM), and human cytokine array

OSCC cells growing in DMEM medium with 10 % FBS were replaced with DMEM medium for 48 h and OSCC-CM was collected. CAFs or NFs culturing in DMEM medium with 10 % FBS was replaced with OSCC -CM. After 48 h, CAF-CM and NF-CM were collected,

centrifuged at 600g for 20 min to remove cellular debris, and stored at −80 °C for use. The relative concentration of 36 cytokines was measured using the Human cytokine array ARY005B (R&D Systems, USA). Cytokines tested included CXCL1, G-CSF, IL-6, IL-8, CXCL12 and MIF.

2.9. Xenografts

5×10^6 SCC47 cells ($DEC2^{hi}$ SCC47 and vector SCC47 cells) mixed with equivalent NFs or CAFs were subcutaneously injected into 4-week-old female BALB/c nude mice and examined every 7 days for tumor appearance. Tumor volume was measured weekly until 35 days after inoculation using the formula (length × $width^2$)/2. Tumor weight was determined by general electronic balance. Animal experiments were approved by the Institutional Ethics Committee of West China Hospital of Stomatology of Sichuan University (approval no. WCHSIRB-D-2021-057).

2.10. Statistical analysis

Results were presented as mean ± standard deviation (SD) and were analyzed and presented by GraphPad Prism 8. Correlations were analyzed using the $\chi 2$ test. Means comparisons were performed using Student's t-test or one-way ANOVA. *$p < 0.05$ were considered statistically significant.

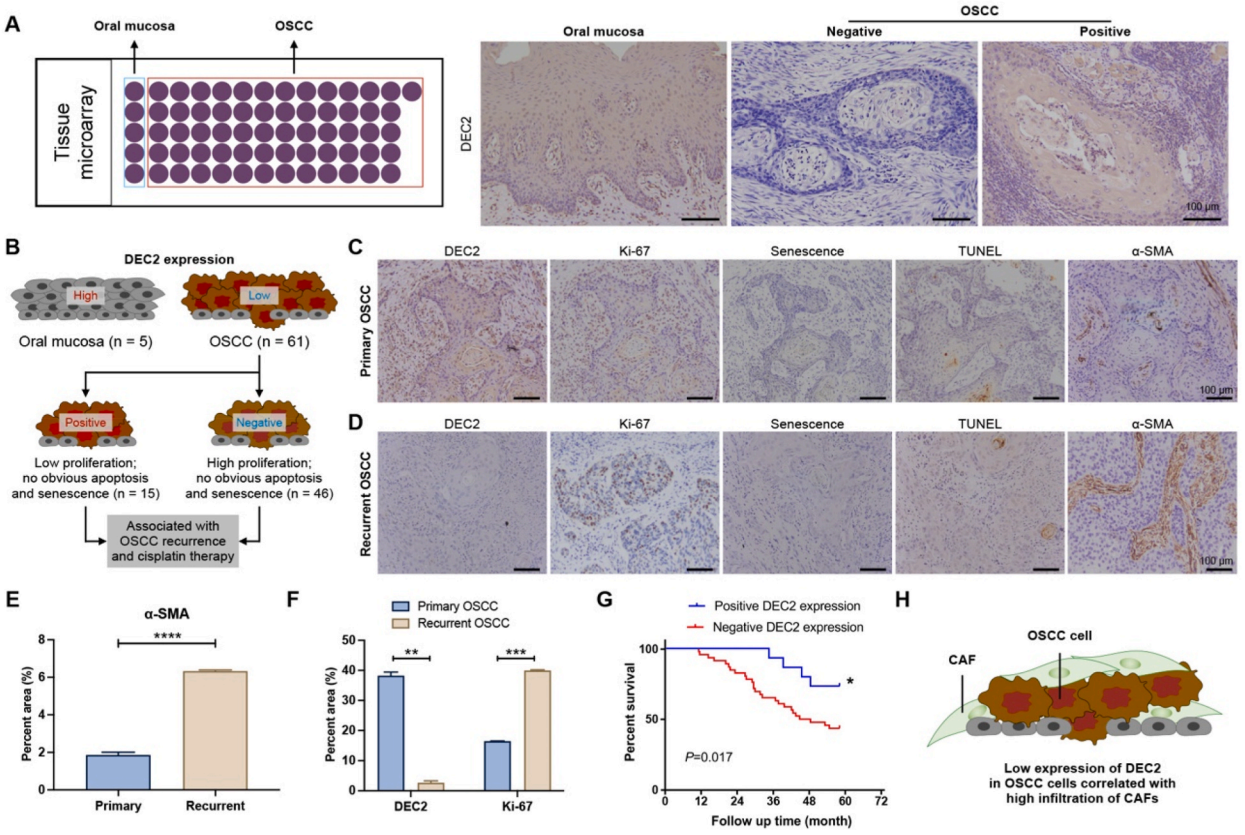

Fig. 1. Expression of DEC2 in OSCC and its association with tumor dormancy. (A) Schematic of tissue microarrays of OSCC tissues (n = 61) and normal mucosal tissues (n = 5) (left panel) and IHC staining of DEC2 (right panel). Scale bars = 100 μm. (B) Schematic representation of DEC2 expression in OSCC tissues. (C and D) In primary (C) and recurrent (D) OSCC tissues, IHC staining was performed to detect the expression of DEC2, Ki-67, and α-SMA, and β-galactosidase and TUNEL staining were used to detect senescence and apoptosis, respectively. Scale bars = 100 μm. (E and F) Quantitative scoring results of α-SMA (E), DEC2 (F), and Ki-67 (F) on IHC staining results. (G) In recurrent OSCC tissues, IHC staining was performed to detect the expression of DEC2, Ki-67, and α-SMA, and β-galactosidase and TUNEL staining were used to detect senescence and apoptosis, respectively. Scale bars = 100 μm. (E) Survival curves of OSCC patients with positive and negative DEC2 expression. (H) Schematic representation of the relationship o between OSCC cells and infiltration of CAFs. Significance level was set as * $p < 0.05$, ** $p < 0.01$, and *** $p < 0.001$.

3. Results

3.1. DEC2 expression relates to cellular dormancy and infiltration of CAFs in OSCC

To investigate the role of DEC2 inOSCC progression, we performed IHC analysis using tissue microarrays (TMA) on 5 normal mucosa and 61 primary OSCC specimens (Fig. 1A). Results showed that DEC2 was predominantly localized in the cytoplasm, and DEC2-positive expression was observed in 3 out of 5 normal oral mucosa cases (60 %) and 15 out of 61 primary OSCC cases (25 %) (Fig. 1A and B). Among the 15 DEC2-positive OSCC cases, 12 cases had a Ki-67 positivity rate of less than 20 %, with negative or weakly positive TUNEL staining and negative β-galactosidase staining (Fig. 1C). In contrast, among the 46 DEC2-negative OSCC cases, 32 cases had a Ki-67 positivity rate of more than 20 %, and all of these 32 cases were weakly positive for TUNEL staining and negative for β-galactosidase staining. The results revealed that OSCC tissues with high expression of DEC2 had low proliferation without obvious apoptosis and senescence (Fig. 1B). Among the 61 OSCC patients included in the tissue microarrays, 30 patients had recurrence. Moreover, we examined α-SMA expression in 30 pairs of primary and recurrent OSCC tissues and assessed its correlation with DEC2 expression (Fig. 1D). Among these 30 patients, 12 were DEC2-positive and 6 were α-SMA-positive in primary foci;, while 4 were DEC2-positive and 24 were α-SMA-positive in recurrent foci (Table S2). Quantitative analysis showed that the expression level of α-SMA was higher in recurrent OSCC tissues than in primary OSCC tissues (Fig. 1E). In addition, the expression of DEC2 was significantly decreased in recurrent OSCC foci compared with primary foci, whereas the expression of Ki-67 was significantly upregulated (Fig. 1F). In addition, clinicopathologic analysis showed that DEC2 expression was closely associated with OSCC recurrence ($p = 0.031$, Table 1) and cisplatin application ($p = 0.006$, Table 1), Kaplan-Meier analysis showed that in patients with primary OSCC, the overall survival rate was higher in the DEC2-positive group than in the negative group ($p = 0.0017$, Fig. 1G). The above results suggest that CAFs mayinteract with DEC2 in OSCC recurrence (Fig. 1H).

3.2. Overexpression of DEC2 induces cellular dormant behavior in OSCC cells

To explore the effect of DEC2 on OSCC cells, we first identified the expression of DEC2 in normal oral keratinocytes (NOK) and OSCC cell lines. The qRT-PCR results revealed a lower level of DEC2 in OSCC cell lines (CAL27 and SCC47) compared with NOK

Table 1
Correlation of DEC2 expression in OSCC with clinical indications.

Clinical Indicators	Number of cases	DEC2		*p*-value
		Negative	Positive	
Gender				0.938
Male	32	24	8	
Female	29	22	7	
Age				0.813
≤55	26	20	6	
>55	35	26	9	
Position				0.382
Tongue	20	12	8	
Buccal	14	12	2	
Gingiva	13	11	2	
Palate	8	7	1	
Floor of mouth	4	3	1	
Pharynx	2	1	1	
T Stage				0.956
1/2	20	15	5	
3/4	41	31	10	
Differentiation level				0.201
High	19	16	3	
Moderate	21	13	8	
Low	21	13	8	
Recurrence				0.031[a]
Yes	30	19	11	
No	31	27	4	
Metastasis				0.820
Yes	11	8	3	
No	50	38	12	
Cisplatin therapy				0.006[a]
Yes	30	18	12	
No	31	28	3	

[a] $p < 0.05$. Abbreviations: OSCC, oral squamous cell carcinoma; DEC2, differentiated Embryonic Chondrocyte gene 2.

(Fig. S1A). Next, we overexpressed DEC2 in CAL27 and SCC47 cells by stable transfection with a DEC2-overexpressing plasmid, confirmed by qRT-PCR and Western blot (Fig. 2A).

Wound-healing results showed that DEC2^{hi} CAL27 and SCC47 cells exhibited a significantly faster wound closure (Fig. 2B and Fig. S1B). Similarly, a significant increase in invasion rates was observed in DEC2^{hi} OSCC cells compared with vector OSCC cells (Fig. 2C and Fig. S1C). These results demonstrated that overexpression of DEC2 promotes the migratory and invasive abilities of OSCC cells *in vitro*. In particular, cancer cell dormancy is characterized by retarded proliferation, temporary G0-G1 arrest, and reduced sensitivity to chemotherapy. Here, CCK-8 assays demonstrated that DEC2^{hi} CAL27 and SCC47 cells displayed a significant reduction of cell proliferation when compared with vector OSCC cells (Fig. 2D). Glucose-consumption assays confirmed that DEC2^{hi} CAL27 and SCC47 cells consumed significantly less glucose in the culture medium than vector groups (Fig. 2E). Flow cytometry analysis demonstrated that the percentage of cells in the G0-G1 phase increased from 20.05 % to 39.77 % in DEC2^{hi} CAL27 cells and from 28.93 % to 47.58 % in DEC2^{hi} SCC47 cells compared with vector groups, which suggests that DEC2^{hi} OSCC cells arrested in G0-G1 phase (Fig. 2F and Fig. S1D). Apoptosis and B-galactosidase staining tests revealed that DEC2 overexpression had no influence on cell apoptosis and senescence (Fig. 2G and H).

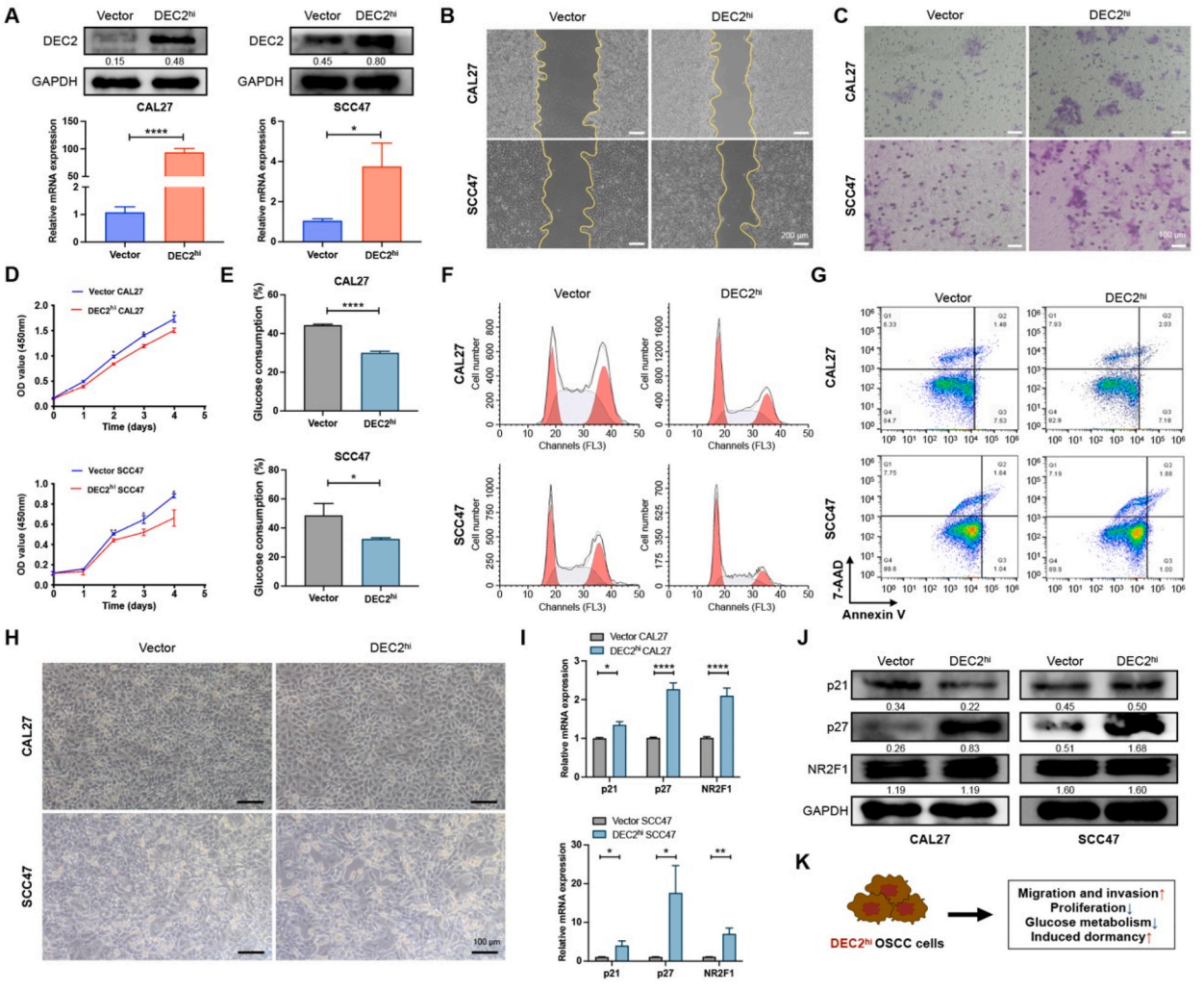

Fig. 2. Overexpression of DEC2 induces dormancy in OSCC cells. (A) qRT-PCR and Western blots verified that the DEC2 overexpression plasmid successfully upregulated DEC2 levels in OSCC cells. The full and non-adjusted images for blots have been provided as supplementary material. (B) Wound healing assays of indicated OSCC cells at 48 h. Scale bars = 200 μm. (C) Transwell invasion assays of indicated OSCC cells. Scale bars, 100 μm. Scale bars = 100 μm. (D) CCK-8 assays were performed to examine the effect of overexpressing DEC2 on the proliferation of OSCC cells. (E) Glucose consumption assay was performed to determine the effect of DEC2 overexpression on glucose metabolism in OSCC cells. (F and G) Flow cytometry assay was performed to detect the effect of DEC2 overexpression on OSCC cell cycle (F) and apoptosis (G). (H) β-galactosidase assay was performed to determine the effect of DEC2 overexpression on OSCC cell senescence. Scale bars = 100 μm. (I and J) qRT-PCR (I) and Western blots (J) showed the expression levels of dormancy markers in OSCC cells after DEC2 overexpression. The full and non-adjusted images for blots have been provided as supplementary material. (K) Schematic representation of the effect of DEC2 on OSCC cells. Significance level was set as * $p < 0.05$, ** $p < 0.01$, *** $p < 0.001$, and **** $p < 0.0001$.

The expression of dormancy markers p21, p27, and Nuclear receptor subfamily 2 group F member 1 (NR2F1) in OSCC cells was further examined after DEC2 overexpression. The qRT-PCR results showed that the expression of *p21*, *p27*, and *NR2F1* in DEC2^{hi} OSCC cells was significantly increased compared with that in the vector group (Fig. 2I). Western blots showed that in the DEC2^{hi} group, the expression of p27 was significantly up-regulated, and there was no significant difference in the expression of p21 and NR2F1 (Fig. 2J). In brief, DEC2 overexpression increased the migration and invasion ability of OSCC cells, decreased their proliferation and glucose metabolism, and induced dormancy of OSCC cells, while it had no significant effect on apoptosis and senescence (Fig. 2K).

3.3. DEC2 induces OSCC cellular dormancy and negative feedback regulation between cisplatin and DEC2

We further assessed the relationship between DEC2 expression and time span of recurrence in samples of OSCC patients treated with cisplatin after tumor resection (Fig. 3A). Intriguingly, 25 % (3/12) of OSCC patients with early recurrence (less than 3 years) had strong DEC2 expression (Table S3). In contrast, 70 % (7/10) of patients who survived more than 5 years had positive DEC2 staining (Table S3). DEC2 was not detected in the tissues of 75 % (6/8) of patients who relapsed between 3 and 5 years, whereas the remaining patients had weak DEC2 expression(Table S3).

In OSCC, cisplatin elevated DEC2 expression in HSC-3 cells, but had little impact on DEC2 expression in CA9-22 cells [19]. Therefore, we examined the regulatory effects of cisplatin on DEC2 expression in CAL27 and SCC47 cells. The half maximal inhibitory concentration (IC50) of cisplatin on CAL27 and SCC47 cells were 2.11 μg/mL and 2.05 μg/mL, respectively (Fig. S2). qRT-PCR and western blots confirmed that cisplatin treatment increased DEC2 expression in CAL27 and SCC47 cells in a dose-dependent manner

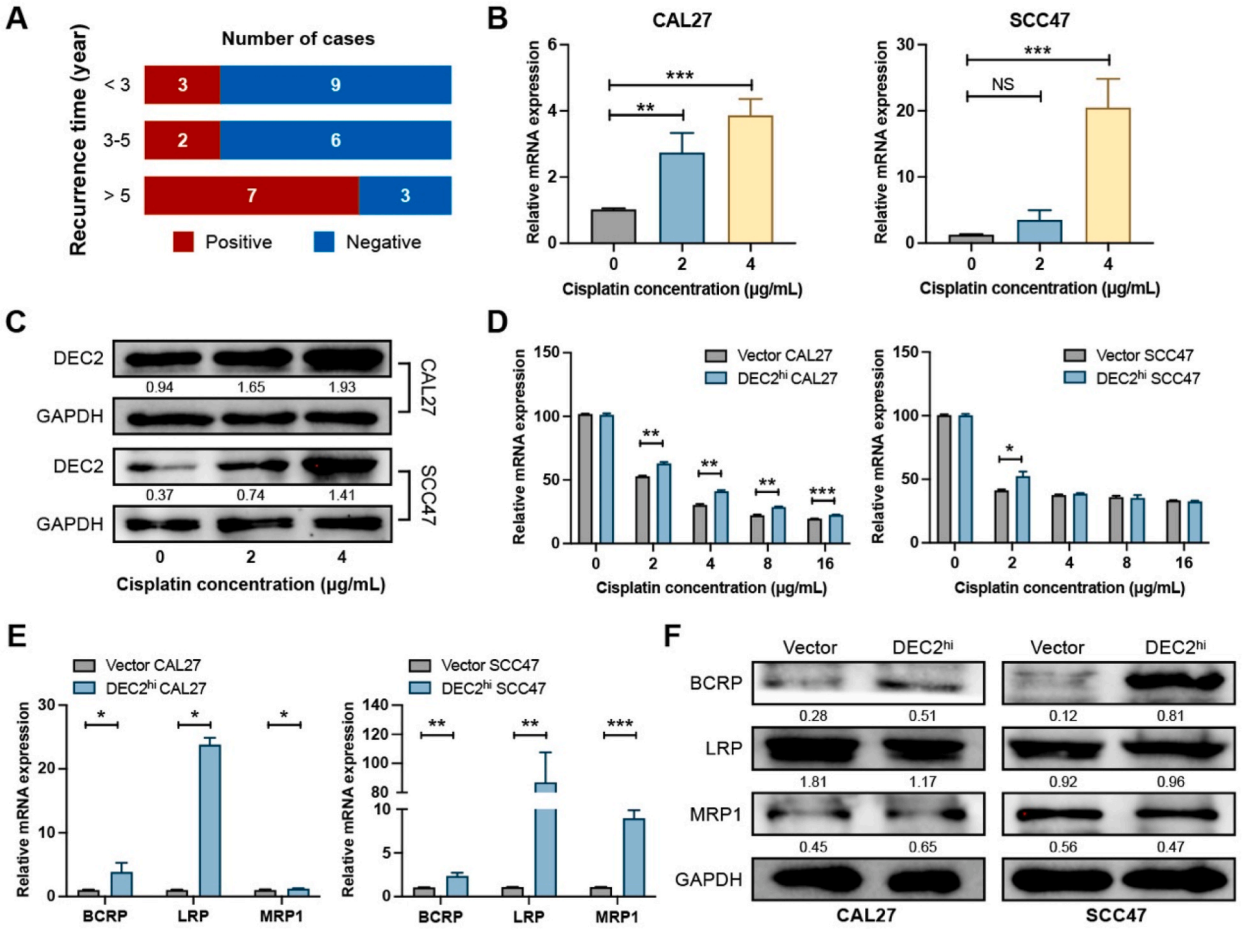

Fig. 3. Interaction of DEC2 with OSCC dormancy and cisplatin utilization. (A) Bar plots demonstrating the relationship between DEC2 expression and recurrence time of OSCC patients. (B and C) qRT-PCR (B) and Western blots (C) showed the expression level of DEC2 in OSCC cells after cisplatin treatment. The full and non-adjusted images for blots have been provided as supplementary material. (D) CCK-8 assay was used to detect the activity of cisplatin treatment on the indicated OSCC cells. (E and F) qRT-PCR (E) and Western blot assay (F) were performed to detect the expression levels of MDR genes in OSCC cells after DEC2 overexpression. The full and non-adjusted images for blots have been provided as supplementary material. Significance level was set as * $p < 0.05$, ** $p < 0.01$, and *** $p < 0.001$. Abbreviations: OSCC, oral squamous cell carcinoma; DEC2, differentiated Embryonic Chondrocyte gene 2. BCRP, breast cancer resistance protein; LRP, lung resistance-related protein; MRP1, multidrug resistance protein-1.

(Fig. 3B and C). Next, we monitored the response of DEC2^{hi} OSCC cells to different concentrations of cisplatin (0, 2, 4, 8, and 16 μg/mL). DEC2^{hi} CAL27 cells showed significantly increased resistance to cisplatin, whereas DEC2^{hi} SCC47 cells showed only resistance to 2 μg/mL cisplatin without obvious change in other groups. (Fig. 3D). Thus, DEC2 overexpression could endow OSCC cells with cisplatin resistance. The multidrug-resistant (MDR) family drug transporters play an important role in chemotherapy response and prognostic judgment in OSCC. To elucidate the MDR phenotype in OSCC, we further analyzed the expression of MDR-related genes, *Breast cancer resistance protein (BCRP), Lung resistance-related protein (LRP), and Multidrug resistance protein-1 (MRP1)* in DEC2^{hi} CAL27 and SCC47 cells. As expected, constitutive expression of DEC2 significantly induced higher levels of each MDR-related gene. qRT-PCR results showed that *LRP* exhibited the most prominent elevation, which was increased by 22.9 folds in DEC2^{hi} CAL27 cells and 111.5 folds in DEC2^{hi} SCC47 cells compared with vector cells (Fig. 3E). Western blots showed that overexpression of DEC2 significantly increased the expression of BCRP in CAL27 and SCC47 cells (Fig. 3F).

3.4. CAFs reactivate DEC2-mediated dormant OSCC cells in vitro

However, whether CAFs get involved in cancer cell dormancy remains unclear. Therefore, we isolated CAFs and NFs from OSCC specimens (Fig. 4A). Immunofluorescent staining and Western Blot confirmed that CAFs exhibited strong positivity for α-SMA and Vimentin compared to NFs (Fig. 4B–D and Figs. S3A and B). Initially, CAFs and NFs were cultured in DEC2^{hi} OSCC-CM for 24 h before replacing the DEC2^{hi} OSCC-CM with DMEM medium. CAF-CM and NF-CM were subsequently collected 48 h later. CCK-8 assay showed that CAF-CM promoted tumor cell proliferation and increased cisplatin resistance of OSCC cells when compared with the NF-CM treatment group (Fig. 4E and F). Furthermore, qRT-PCR results showed that CAF-CM treatment could down-regulate the expression

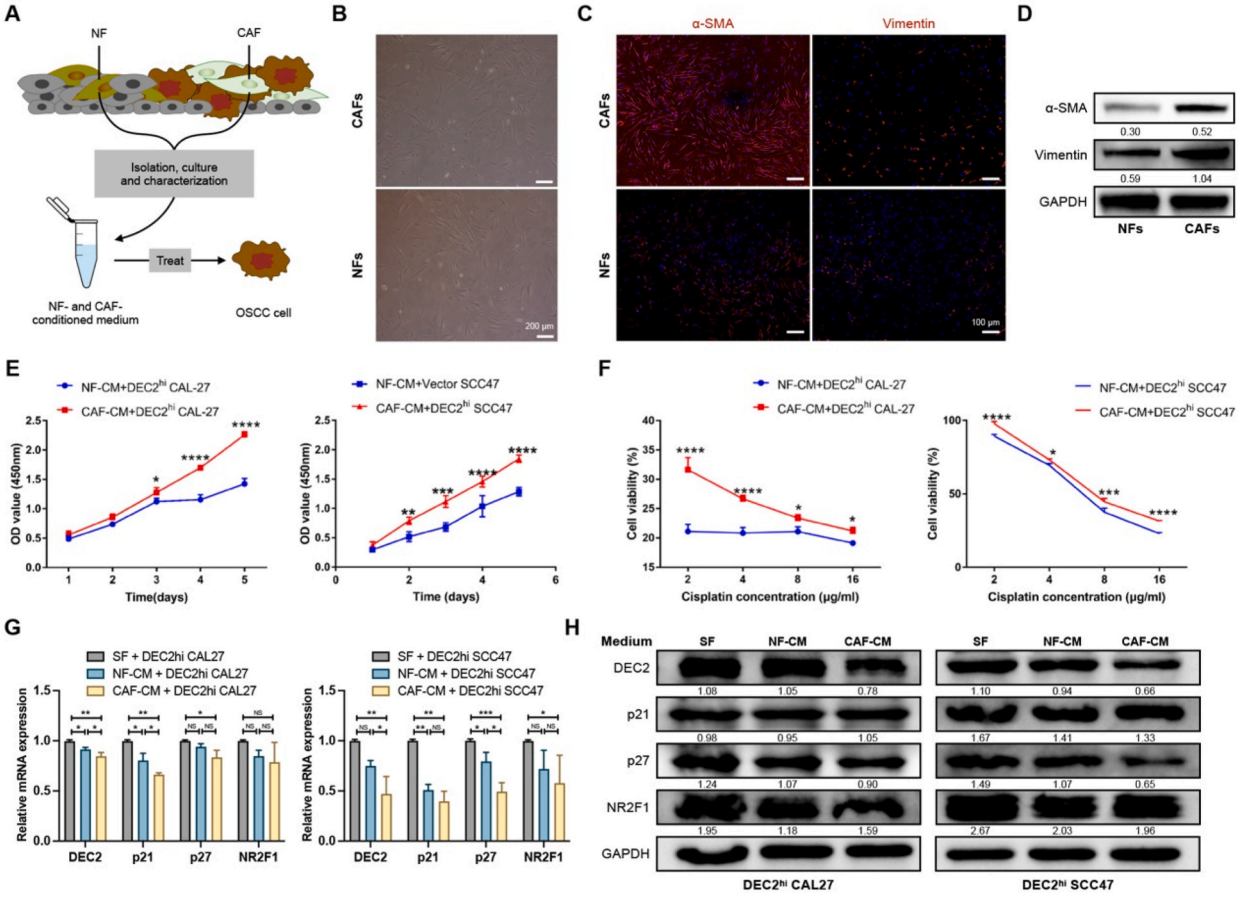

Fig. 4. CAFs awaken DEC2-induced OSCC dormancy. (A) Schematic diagram showing the isolation of CAFs and NFs from OSCC specimens and the treatment of OSCC cells with CAFs- and NFs-CM. (B) Microscopy images of CAFs and NFs from OSCC specimens. Scale bars = 200 μm. (C and D) Immunofluorescence staining (C) and Western blots (D) showed that α-SMA and vimentin were expressed higher in CAFs than in NFs. Scale bars = 100 μm. The full and non-adjusted images for blots have been provided as supplementary material. (E and F) CCK-8 assay was used to examine the effects of NF-CM and CAF-CM on the activity of DEC2^{hi} OSCC cells (E) as well as the cell activity under cisplatin treatment (F). (G and H) qRT-PCR (G) and Western blots (H) showed the expression levels of DEC2^{hi} OSCC cell dormancy markers under SF, NF-CM, and CAF-CM. The full and non-adjusted images for blots have been provided as supplementary material. Significance level was set as * $p < 0.05$, ** $p < 0.01$, *** $p < 0.001$, and **** $p < 0.0001$. Abbreviations: NF, normal fibroblasts; CAF, cancer-associated fibroblast; CM, conditioned medium; SF, serum-free.

of *DEC2*, *p21*, and *p27*, but had no significant effect on *NR2F1* (Fig. 4G). Western blots showed that CAF-CM treatment slightly downregulated the expression of DEC2, p27, and NR2F1, but there was no significant change in p21 (Fig. 4H).

3.5. CAFs-derived CXCL1 reactivates cellular dormancy in OSCC

Furthermore, we used a human cytokine array to identify the significantly dysregulated cytokines between CAF-CM and NF-CM (Fig. 5A). As shown, the numbers 1–6 represent CXCL1, G-CSF, IL-6, IL-8, CXCL12, and MIF, respectively. Compared to NF-CM, the expression of three cytokines (CXCL1, IL-6, and IL-8) was significantly upregulated in CAF-CM, with a slight increase in G-CSF and a slight downregulation of CXCL12 and MIF (Fig. 5B and C). qRT-PCR results confirmed that CXCL1 and IL-6 were remarkably increased in CAF-CM when compared to NF-CM (Fig. 5D). Next, we tested whether IL-6 or CXCL1 mediated the growth increase induced by CAF-CM. OSCC cells were exposed to different concentrations (62.5–1000 ng/mL) of recombinant IL-6 or CXCL1 for 24 h, which impacts cell proliferation were evaluated by CCK-8 assay. Compared with serum-free (SF) medium, CXCL1 at 1000 ng/mL significantly promoted the proliferation of CAL27 and SCC47 cells, which was comparable to CAF-CM (Fig. 5E). On the other hand, IL-6 at 1000 ng/mL could only significantly increase the growth of SCC47 cells compared to SF, which was inferior to equivalent CXCL1 or CAF-CM (Fig. 5D). Furthermore, treatment with 1000 ng/mL CXCL1 significantly inhibited the DEC2 expression relative to SF, while application of CXCR2 blocker SB225002 rescued the level of DEC2 (Fig. 5F and G).

3.6. CAFs reactivated DEC2-induced dormancy in OSCC nude mice

To validate the effect of CAFs on dormancy of OSCC cells, DEC2^{hi} and vector SCC47 cells were mixed with equal amounts of NFs or CAFs and subcutaneously injected into 4-week-old female BALB/c nude mice (Fig. 6A and B). Among all 4 groups, the fastest tumor growth was observed in the CAF + DEC2^{hi} group ($p < 0.001$, Fig. 6C). The mean tumor weights of CAF + DEC2^{hi}, CAF + vector, NF + vector, and NF + DEC2^{hi} groups were 0.2773 ± 0.02487 g, 0.1697 ± 0.03687 g, 0.1486 ± 0.0296 g, and 0.05948 ± 0.01602 g, respectively (Fig. 6D). Compared with the NF + vector group, the mean tumor weight of the CAF + DEC2^{hi} group was remarkably enhanced ($p < 0.05$), while those of the CAF + vector group and NF + vector group had no statistical difference ($p > 0.05$, Fig. 6D). We further examined the expression of DEC2 and α-SMA in xenograft tumors. Consistently with *in vitro* results, compared with the CAF + vector group, the expressions of DEC2 were significantly decreased in the xenograft tumor tissues of CAF + DEC2^{hi} group ($p < 0.05$), whereas the expressions of α-SMA was significantly increased ($p < 0.05$, Fig. 6E and F). Furthermore, qRT-PCR results showed that the expression of dormancy markers (p21, p27, and NR2F1) were significantly decreased in the xenograft tumor tissues of CAF + DEC2^{hi} group compared with the NF + DEC2^{hi} group ($p < 0.01$, Fig. 6G).

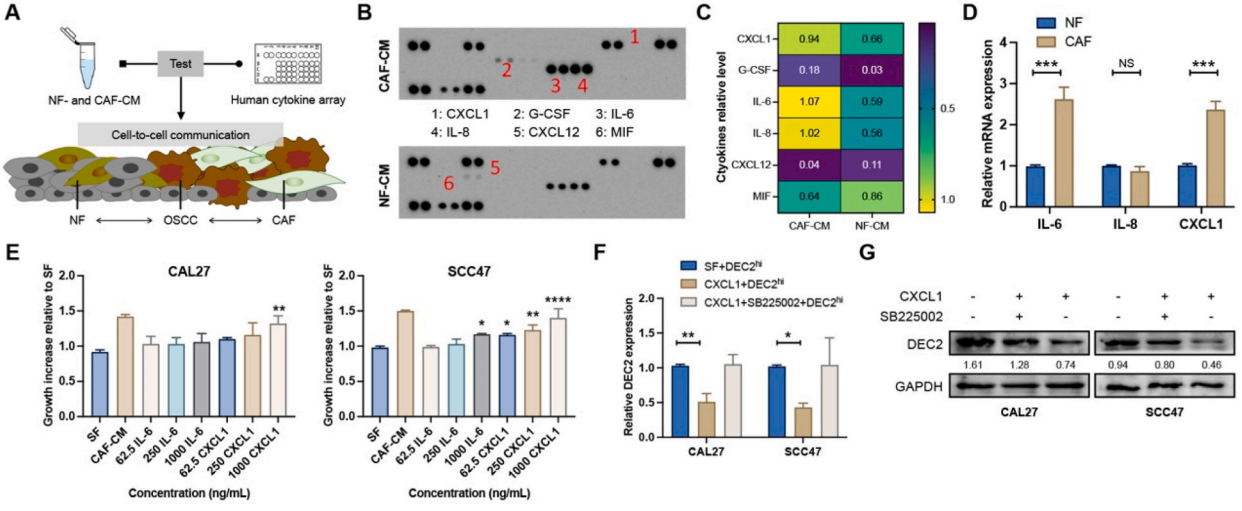

Fig. 5. CAF-derived CXCL1 awakens DEC2-induced dormancy. (A) Schematic representation of cytokine detection by human cytokine array after CAFs- and NFs-CM treatment of OSCC cells. (B) The human cytokine array showed the expression levels of different cytokines after CAFs- and NFs-CM treatment of OSCC cells. (C) The pixel densities of the specified cytokines in the array were normalized and quantified. (D) Expression of IL-6, IL-8, and CXCL1 in CAF and NF verified by qRT-PCR. (E) CCK-8 assay was used to examine the effects of SF, CAF-CM, and different concentrations of IL-6 and CXCL1 on the proliferative ability of OSCC cells. (F and G) qRT-PCR (F) and Western blots (G) showed the expression levels of DEC2 after treatment of DEC2^{hi} OSCC cells with CXCL1 and SB225002. The full and non-adjusted images for blots have been provided as supplementary material. Significance level was set as * $p < 0.05$, ** $p < 0.01$, *** $p < 0.001$, and **** $p < 0.0001$. Abbreviations: NF, normal fibroblasts; CAF, cancer-associated fibroblast; CM, conditioned medium; SF, serum-free.

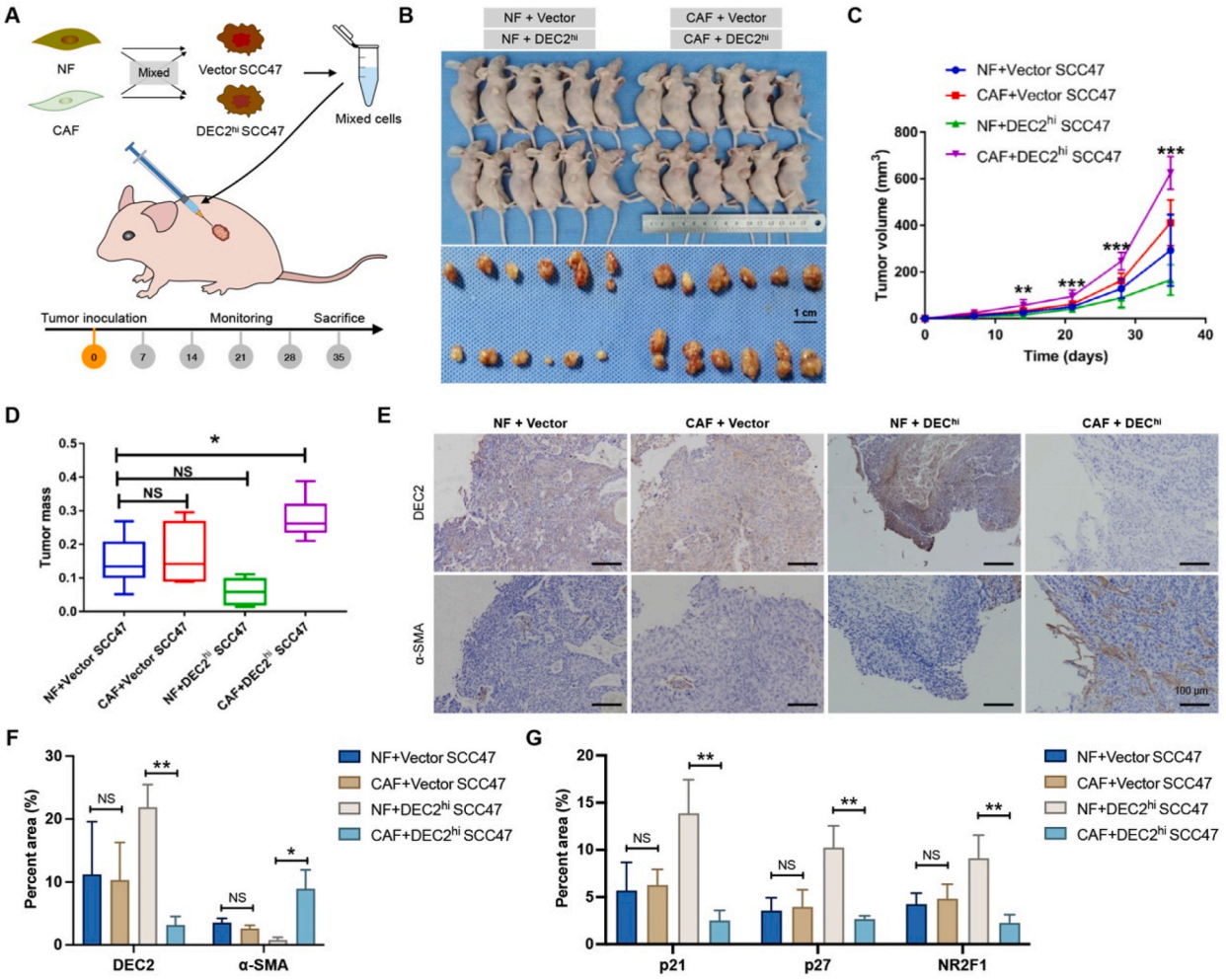

Fig. 6. CAFs reactivated DEC2-induced dormancy *in vivo*. (A) Schematic illustration of the experimental route of NF and CAF mixed with DEC2^{hi} and vector OSCC cells inoculated in nude mice. (B) Body and tumor photographs of nude mice after sacrifice. Scale = 1 cm. (C) Tumor volume of nude mice. (D) Tumor mass of nude mice. (E and F) IHC staining (E) and quantitative scoring (F) results of DEC2 and α-SMA in the indicated groups. Scale bar = 100 μm. (G) qRT-PCR showed the expression levels of cell dormancy markers in the indicated groups. Significance level was set as * $p < 0.05$, ** $p < 0.01$, and *** $p < 0.001$.

4. Discussion

Cancer dormancy plays a decisive role in the recurrence and metastasis of various cancers. Here, IHC staining of 61 OSCC patients revealed that 26 of them showed low proliferation and no significant apoptosis or senescence in their OSCC tissues, indicating a possible dormant state. In particular, 80 % (12 out of 15) of DEC2-positively expressing OSCC tissues showed dormancy, suggesting a strong correlation between DEC2 and dormancy. *In vitro*, DEC2^{hi} CAL27 and SCC47 cells showed increased G0-G1 arrest, reduced glucose consumption, and enhanced resistance to cisplatin, indicating cellular dormancy. DEC2 overexpression also induced the expression of NR2F1, p21, and p27, which are well-recognized markers of dormancy. Additionally, our study found that exposure to cisplatin was capable of up-regulating the DEC2 expression in CAL27 and SCC47 cells. This is consistent with the fact, chemotherapeutic agents (such cisplatin and paclitaxel) can up-regulate DEC2 expression in OSCC cells (HSC-3) as well as breast cancer cells (MCF-7), which may contribute to the DEC2-mediated cancer dormancy [20,19].

Our analysis of OSCC tissues showed that DEC2 expression was associated with cisplatin and tumor relapse. Multidrug resistance-related genes play a vital role in the development of resistance to chemotherapeutic agents. To better investigate the mechanisms of DEC2-mediated chemoresistance in OSCC, we analyzed the expression of MDR-related genes: BCRP, LRP, and MRP1. qRT-PCR results showed that LRP had the highest upregulation in both DEC2^{hi} CAL27 and SCC47 cells. Previous studies revealed that the LRP promoter contains multiple binding sites for transcription factors, such as STAT and E-box. Ryuji et al. suggested that USF1 binding to an E-box element may be critical for basal MVP/LRP promoter activation by chromatin immunoprecipitation assay [21]. Given that DEC2 preferentially binds to E-box elements to regulate the transcription of target genes, we speculated that DEC2 might evoke the

expression of LRP in an E-box element-dependent manner, thereby conferring cisplatin resistance in OSCC cells. The gene expression levels of LRP and MRP1 were inconsistent with the changes in protein levels, which may be due to suppressed translational efficiency of LRP and MRP1. In addition, BCRP mRNA and protein levels were upregulated in both DEC2^{hi} CAL27 and SCC47 cells, which was consistent with the finding that the regulation of BCRP expression was mediated by DEC2.

Cancer cell dormancy is determined by not only cell intrinsic characteristics, but also extrinsic influences from normal components in the TME, for example, mesenchymal stem cells (MSCs), endothelial cells (ECs), and immune cells [22]. However, as the most predominant stromal cell in the TME, the association between CAFs and cellular dormancy remains unexplored. Scholars have suggested that CAFs may regulate cancer cell dormancy by ECM remodeling or metabolic crosstalk [23]. Mounting evidence has pointed out that tumor progression highly relies on the reciprocal communication between CAFs and tumor cells, mediated by direct cell-cell contact, secreted soluble factors, and extracellular vesicles [24]. To date, there is insufficient evidence to support the association between CAFs and cancer cell dormancy or reactivation. However, based on following circumstantial evidence, it can be speculated that CAFs may play a pivotal role in cancer cell dormancy or reactivation: (1) Ghajar et al. utilized murine, zebrafish and organotypic models to demonstrate that endothelial tip cell-derived POSTN reactivated cellular dormancy in breast cancer, which is mainly released by CAFs in the TME [25–27]; (2) CAFs could modulate ECM density and composition to manipulate its stiffness and degradation. Moreover, reducing environmental stiffness induces cellular dormancy, whereas increasing stiffness facilitates dormancy reactivation in hepatocellular carcinoma [28,29]; (3) In the presence of growth factors, cytokines, and cell-matrix proteins, ARHI could up-regulate the autophagy levels of autophagy in ovarian cancer cells and promote cellular dormancy [30]. Recent "metabolic symbiosis" studies proposed that cancer cells stimulate a rise of autophagy in CAFs, which in turn provides nutrients to support their metabolic needs and reduce their autophagy needs [31]. In addition, IL-6, primarily produced by CAFs in TME, has been confirmed to down-regulate the expression of ARH1 and the autophagy of ovarian cancer cells, thereby reactivating dormant ovarian cancer cells [32–34]. Here we showed that CAFs-derived CXCL1 promoted the exit of dormancy in OSCC cells. It was observed that NF-CM also had less CXCL1 also and therefore also weakly inhibited the expression of dormant genes in OSCC cells. The published literature has demonstrated that both NFs and CAFs are capable of secreting molecules that have the potential to facilitate tumor invasion and metastasis [35–37]. Current evidence supports the notion that CXCL1 was highly expressed in the TME and implicated in cancer progression and inflammation [38–40]. Previous studies verified that treatment of OSCC cell lines with CXCL1 could induce intracellular ERK phosphorylation, leading to their enhanced proliferation, migration and invasion [41,42]. In line with aforementioned evidence, we found that CAFs-derived CXCL1 repressed DEC2 expression, which was responsible for the escape from dormancy and subsequent outgrowth of OSCC.

Taken together, we found that DEC2 overexpression led to cellular dormancy and cisplatin resistance in OSCC. Additionally, CAFs-derived CXCL1 inhibited the DEC2 expression, therefore inducing the exit of dormancy in DEC2-overexpressing OSCC cells. Recasens et al. proposed three strategies to target cancer cell dormancy: 1) to maintain cancer cell dormancy; 2) to reactivate dormant cells and increase their susceptibility to anti-proliferative drugs; and (iii) to eliminate dormant cancer cells [5]. In the context of OSCC, we could up-regulate DEC2 and block the release of CXCL1 in TME to maintain cancer cells in a dormant state. Alternatively, we may promote the CXCL1 secretion in the TME and co-application of chemotherapeutic drugs to kill dormant cancer cells. Thus, further investigation is needed to explore the treatment effect and side effects of these strategies *in vivo*.

In conclusion, high levels of DEC2 can induce tumor cell dormancy and the occurrence of cisplatin resistance, which is significantly associated with tumor recurrence and infiltration of cancer-associated fibroblasts in OSCC. CAFs can secrete CXCL1, thereby down-regulating the expression of DEC2 in tumor cells and reactivating dormant OSCC cells. Therefore, DEC2 is expected to become a promising marker for cellular dormancy, sustained tumor chemosensitivity, and recurrence of OSCC, providing a new target for clinical targeted therapy.

CRediT authorship contribution statement

Wei-long Zhang: Writing – original draft, Software, Resources, Methodology, Investigation, Data curation. **Hua-yang Fan:** Writing – review & editing, Visualization, Validation. **Bin-jun Chen:** Validation. **Hao-fan Wang:** Validation. **Xin Pang:** Formal analysis. **Mao Li:** Investigation. **Xin-hua Liang:** Funding acquisition, Conceptualization. **Ya-ling Tang:** Supervision, Funding acquisition, Conceptualization.

Data availability statement

All of the data are available in all Tables and Figures of the manuscripts.

Declaration of competing interest

The authors declare that they have no known competing financial interests or personal relationships that could have appeared to influence the work reported in this paper.

Acknowledgements

This research was funded by National Natural Science Foundation of China grants (Nos. 81972542, 82073000, and 82173326) and Interdisciplinary Innovation Project of West China College of Stomatology, Sichuan University (RD-03-202004).

Appendix A. Supplementary data

Supplementary data to this article can be found online at https://doi.org/10.1016/j.heliyon.2024.e39133.

References

[1] Y. Tan, Z. Wang, M. Xu, B. Li, Z. Huang, S. Qin, E.C. Nice, J. Tang, C. Huang, Oral squamous cell carcinomas: state of the field and emerging directions, Int. J. Oral Sci. 15 (2023) 44, https://doi.org/10.1038/s41368-023-00249-w.

[2] H. Shimomura, T. Sasahira, C. Nakashima, M. Kurihara-Shimomura, T. Kirita, Non-SMC condensin I complex subunit H (NCAPH) is associated with lymphangiogenesis and drug resistance in oral squamous cell carcinoma, J. Clin. Med. 9 (2019), https://doi.org/10.3390/jcm9010072.

[3] M.D. Mody, J.W. Rocco, S.S. Yom, R.I. Haddad, N.F. Saba, Head and neck cancer, Lancet 398 (2021) 2289–2299, https://doi.org/10.1016/s0140-6736(21)01550-6.

[4] A.T. Ruffin, H. Li, L. Vujanovic, D.P. Zandberg, R.L. Ferris, T.C. Bruno, Improving head and neck cancer therapies by immunomodulation of the tumour microenvironment, Nat. Rev. Cancer 23 (2023) 173–188, https://doi.org/10.1038/s41568-022-00531-9.

[5] A. Recasens, L. Munoz, Targeting cancer cell dormancy, Trends Pharmacol. Sci. 40 (2019) 128–141, https://doi.org/10.1016/j.tips.2018.12.004.

[6] X.L. Gao, M. Zhang, Y.L. Tang, X.H. Liang, Cancer cell dormancy: mechanisms and implications of cancer recurrence and metastasis, OncoTargets Ther. 10 (2017) 5219–5228, https://doi.org/10.2147/ott.S140854.

[7] T.G. Phan, P.I. Croucher, The dormant cancer cell life cycle, Nat. Rev. Cancer 20 (2020) 398–411, https://doi.org/10.1038/s41568-020-0263-0.

[8] Y. Chhabra, A.T. Weeraratna, Fibroblasts in cancer: unity in heterogeneity, Cell 186 (2023) 1580–1609, https://doi.org/10.1016/j.cell.2023.03.016.

[9] X. Chen, E. Song, Turning foes to friends: targeting cancer-associated fibroblasts, Nat. Rev. Drug Discov. 18 (2019) 99–115, https://doi.org/10.1038/s41573-018-0004-1.

[10] C. Thuwajit, A. Ferraresi, R. Titone, P. Thuwajit, C. Isidoro, The metabolic cross-talk between epithelial cancer cells and stromal fibroblasts in ovarian cancer progression: autophagy plays a role, Med. Res. Rev. 38 (2018) 1235–1254, https://doi.org/10.1002/med.21473.

[11] S. Honma, T. Kawamoto, Y. Takagi, K. Fujimoto, F. Sato, M. Noshiro, Y. Kato, K. Honma, Dec1 and Dec2 are regulators of the mammalian molecular clock, Nature 419 (2002) 841–844, https://doi.org/10.1038/nature01123.

[12] K. Miyazaki, T. Kawamoto, K. Tanimoto, M. Nishiyama, H. Honda, Y. Kato, Identification of functional hypoxia response elements in the promoter region of the DEC1 and DEC2 genes, J. Biol. Chem. 277 (2002) 47014–47021, https://doi.org/10.1074/jbc.M204938200.

[13] T. Hu, N. He, Y. Yang, C. Yin, N. Sang, Q. Yang, DEC2 expression is positively correlated with HIF-1 activation and the invasiveness of human osteosarcomas, J. Exp. Clin. Cancer Res. 34 (2015) 22, https://doi.org/10.1186/s13046-015-0135-8.

[14] H. Li, X. Ma, D. Xiao, Y. Jia, Y. Wang, Expression of DEC2 enhances chemosensitivity by inhibiting STAT5A in gastric cancer, J. Cell. Biochem. 120 (2019) 8447–8456, https://doi.org/10.1002/jcb.28131.

[15] P. Bragado, Y. Estrada, F. Parikh, S. Krause, C. Capobianco, H.G. Farina, D.M. Schewe, J.A. Aguirre-Ghiso, TGF-β2 dictates disseminated tumour cell fate in target organs through TGF-β-RIII and p38α/β signalling, Nat. Cell Biol. 15 (2013) 1351–1361, https://doi.org/10.1038/ncb2861.

[16] Y. Liu, F. Sato, T. Kawamoto, K. Fujimoto, S. Morohashi, H. Akasaka, J. Kondo, Y. Wu, M. Noshiro, Y. Kato, H. Kijima, Anti-apoptotic effect of the basic helix-loop-helix (bHLH) transcription factor DEC2 in human breast cancer cells, Gene Cell. 15 (2010) 315–325, https://doi.org/10.1111/j.1365-2443.2010.01381.x.

[17] E. Giannoni, M.L. Taddei, A. Morandi, G. Comito, M. Calvani, F. Bianchini, B. Richichi, G. Raugei, N. Wong, D. Tang, P. Chiarugi, Targeting stromal-induced pyruvate kinase M2 nuclear translocation impairs oxphos and prostate cancer metastatic spread, Oncotarget 6 (2015) 24061–24074, https://doi.org/10.18632/oncotarget.4448.

[18] X. Yang, J.S. Wu, M. Li, W.L. Zhang, X.L. Gao, H.F. Wang, X.H. Yu, X. Pang, M. Zhang, X.H. Liang, Y.L. Tang, Inhibition of DEC2 is necessary for exiting cell dormancy in salivary adenoid cystic carcinoma, J. Exp. Clin. Cancer Res. 40 (2021) 169, https://doi.org/10.1186/s13046-021-01956-0.

[19] Y. Wu, F. Sato, U.K. Bhawal, T. Kawamoto, K. Fujimoto, M. Noshiro, H. Seino, S. Morohashi, Y. Kato, H. Kijima, BHLH transcription factor DEC2 regulates pro-apoptotic factor Bim in human oral cancer HSC-3 cells, Biomed Res 33 (2012) 75–82, https://doi.org/10.2220/biomedres.33.75.

[20] Y. Wu, F. Sato, U.K. Bhawal, T. Kawamoto, K. Fujimoto, M. Noshiro, S. Morohashi, Y. Kato, H. Kijima, Basic helix-loop-helix transcription factors DEC1 and DEC2 regulate the paclitaxel-induced apoptotic pathway of MCF-7 human breast cancer cells, Int. J. Mol. Med. 27 (2011) 491–495, https://doi.org/10.3892/ijmm.2011.617.

[21] R. Ikeda, Y. Nishizawa, Y. Tajitsu, K. Minami, H. Mataki, S. Masuda, T. Furukawa, S. Akiyama, K. Yamada, Y. Takeda, Regulation of major vault protein expression by upstream stimulating factor 1 in SW620 human colon cancer cells, Oncol. Rep. 31 (2014) 197–201, https://doi.org/10.3892/or.2013.2818.

[22] D. Senft, I. Jeremias, Tumor cell dormancy-triggered by the niche, Dev. Cell 49 (2019) 311–312, https://doi.org/10.1016/j.devcel.2019.04.022.

[23] A.L. Parker, T.R. Cox, The role of the ECM in lung cancer dormancy and outgrowth, Front. Oncol. 10 (2020) 1766, https://doi.org/10.3389/fonc.2020.01766.

[24] P. Cirri, P. Chiarugi, Cancer associated fibroblasts: the dark side of the coin, Am. J. Cancer Res. 1 (2011) 482–497.

[25] C.M. Ghajar, H. Peinado, H. Mori, I.R. Matei, K.J. Evason, H. Brazier, D. Almeida, A. Koller, K.A. Hajjar, D.Y. Stainier, E.I. Chen, D. Lyden, M.J. Bissell, The perivascular niche regulates breast tumour dormancy, Nat. Cell Biol. 15 (2013) 807–817, https://doi.org/10.1038/ncb2767.

[26] K. Ratajczak-Wielgomas, J. Grzegrzolka, A. Piotrowska, A. Gomulkiewicz, W. Witkiewicz, P. Dziegiel, Periostin expression in cancer-associated fibroblasts of invasive ductal breast carcinoma, Oncol. Rep. 36 (2016) 2745–2754, https://doi.org/10.3892/or.2016.5095.

[27] L. Chu, F. Wang, W. Zhang, H.F. Li, J. Xu, X.W. Tong, Periostin secreted by carcinoma-associated fibroblasts promotes ovarian cancer cell platinum resistance through the PI3K/akt signaling pathway, Technol. Cancer Res. Treat. 19 (2020) 1533033820977535, https://doi.org/10.1177/1533033820977535.

[28] M. Najafi, B. Farhood, K. Mortezaee, Extracellular matrix (ECM) stiffness and degradation as cancer drivers, J. Cell. Biochem. 120 (2019) 2782–2790, https://doi.org/10.1002/jcb.27681.

[29] J. Schrader, T.T. Gordon-Walker, R.L. Aucott, M. van Deemter, A. Quaas, S. Walsh, D. Benten, S.J. Forbes, R.G. Wells, J.P. Iredale, Matrix stiffness modulates proliferation, chemotherapeutic response, and dormancy in hepatocellular carcinoma cells, Hepatology 53 (2011) 1192–1205, https://doi.org/10.1002/hep.24108.

[30] Z. Lu, R.Z. Luo, Y. Lu, X. Zhang, Q. Yu, S. Khare, S. Kondo, Y. Kondo, Y. Yu, G.B. Mills, W.S. Liao, R.C. Bast Jr., The tumor suppressor gene ARHI regulates autophagy and tumor dormancy in human ovarian cancer cells, J. Clin. Invest. 118 (2008) 3917–3929, https://doi.org/10.1172/jci35512.

[31] C.M. Sousa, D.E. Biancur, X. Wang, C.J. Halbrook, M.H. Sherman, L. Zhang, D. Kremer, R.F. Hwang, A.K. Witkiewicz, H. Ying, J.M. Asara, R.M. Evans, L. C. Cantley, C.A. Lyssiotis, A.C. Kimmelman, Pancreatic stellate cells support tumour metabolism through autophagic alanine secretion, Nature 536 (2016) 479–483, https://doi.org/10.1038/nature19084.

[32] A. Ferraresi, S. Phadngam, F. Morani, A. Galetto, O. Alabiso, G. Chiorino, C. Isidoro, Resveratrol inhibits IL-6-induced ovarian cancer cell migration through epigenetic up-regulation of autophagy, Mol. Carcinog. 56 (2017) 1164–1181, https://doi.org/10.1002/mc.22582.

[33] L. Wang, F. Zhang, J.Y. Cui, L. Chen, Y.T. Chen, B.W. Liu, CAFs enhance paclitaxel resistance by inducing EMT through the IL-6/JAK2/STAT3 pathway, Oncol. Rep. 39 (2018) 2081–2090, https://doi.org/10.3892/or.2018.6311.

[34] N. Erez, S. Glanz, Y. Raz, C. Avivi, I. Barshack, Cancer associated fibroblasts express pro-inflammatory factors in human breast and ovarian tumors, Biochem. Biophys. Res. Commun. 437 (2013) 397–402, https://doi.org/10.1016/j.bbrc.2013.06.089.

[35] J.L. Hu, W. Wang, X.L. Lan, Z.C. Zeng, Y.S. Liang, Y.R. Yan, F.Y. Song, F.F. Wang, X.H. Zhu, W.J. Liao, W.T. Liao, Y.Q. Ding, L. Liang, CAFs secreted exosomes promote metastasis and chemotherapy resistance by enhancing cell stemness and epithelial-mesenchymal transition in colorectal cancer, Mol. Cancer 18 (2019) 91, https://doi.org/10.1186/s12943-019-1019-x.

[36] G. Liu, J. Sun, Z.F. Yang, C. Zhou, P.Y. Zhou, R.Y. Guan, B.Y. Sun, Z.T. Wang, J. Zhou, J. Fan, S.J. Qiu, Y. Yi, Cancer-associated fibroblast-derived CXCL11 modulates hepatocellular carcinoma cell migration and tumor metastasis through the circUBAP2/miR-4756/IFIT1/3 axis, Cell Death Dis. 12 (2021) 260, https://doi.org/10.1038/s41419-021-03545-7.
[37] Z. Zhou, Q. Zhou, X. Wu, S. Xu, X. Hu, X. Tao, B. Li, J. Peng, D. Li, L. Shen, Y. Cao, L. Yang, VCAM-1 secreted from cancer-associated fibroblasts enhances the growth and invasion of lung cancer cells through AKT and MAPK signaling, Cancer Lett. 473 (2020) 62–73, https://doi.org/10.1016/j.canlet.2019.12.039.
[38] Y. Cheng, X.L. Ma, Y.Q. Wei, X.W. Wei, Potential roles and targeted therapy of the CXCLs/CXCR2 axis in cancer and inflammatory diseases, Biochim. Biophys. Acta Rev. Canc 1871 (2019) 289–312, https://doi.org/10.1016/j.bbcan.2019.01.005.
[39] Y. Lu, B. Dong, F. Xu, Y. Xu, J. Pan, J. Song, J. Zhang, Y. Huang, W. Xue, CXCL1-LCN2 paracrine axis promotes progression of prostate cancer via the Src activation and epithelial-mesenchymal transition, Cell Commun. Signal. 17 (2019) 118, https://doi.org/10.1186/s12964-019-0434-3.
[40] A. Zou, D. Lambert, H. Yeh, K. Yasukawa, F. Behbod, F. Fan, N. Cheng, Elevated CXCL1 expression in breast cancer stroma predicts poor prognosis and is inversely associated with expression of TGF-β signaling proteins, BMC Cancer 14 (2014) 781, https://doi.org/10.1186/1471-2407-14-781.
[41] S.A. Khurram, L. Bingle, B.M. McCabe, P.M. Farthing, S.A. Whawell, The chemokine receptors CXCR1 and CXCR2 regulate oral cancer cell behaviour, J. Oral Pathol. Med. 43 (2014) 667–674, https://doi.org/10.1111/jop.12191.
[42] L.Y. Wei, J.J. Lee, C.Y. Yeh, C.J. Yang, S.H. Kok, J.Y. Ko, F.C. Tsai, J.S. Chia, Reciprocal activation of cancer-associated fibroblasts and oral squamous carcinoma cells through CXCL1, Oral Oncol. 88 (2019) 115–123, https://doi.org/10.1016/j.oraloncology.2018.11.002.